Antibacterial Activity and Characteristics of Silver Nanoparticles Biosynthesized From *Carduus Crispus*

Enerelt Urnukhsaikhan
Laboratory of Molecular and Cellular Biophysics, Department of Biology, National University of Mongolia

Bum-Erdene Bold
Laboratory of Molecular and Cellular Biophysics, Department of Biology, National University of Mongolia

Aminaa Gunbileg
Laboratory of Molecular and Cellular Biophysics, Department of Biology, National University of Mongolia

Nominchimeg Sukhbaatar
Laboratory of Molecular and Cellular Biophysics, Department of Biology, National University of Mongolia

Tsogbadrakh Mishig-Ochir (tsogm@num.edu.mn)
Laboratory of Molecular and Cellular Biophysics, Department of Biology, National University of Mongolia

Research Article

Keywords: Antibacterial activity, silver nanoparticles, Carduus crispus, synthesizing metal nanoparticles, AgNP

Posted Date: May 27th, 2021

DOI: https://doi.org/10.21203/rs.3.rs-537949/v1

Abstract

Recently, synthesizing metal nanoparticles using plants has been extensively studied and recognized as a non-toxic and efficient way for biomedical field. The aim of this study is to investigate the role of different parts of *Carduus crispus* medical plant on synthesizing silver nanoparticles and their characteristics. Our study showed that silver nanoparticles (AgNP) synthesized via whole plant extract exhibited a blue shift in absorption spectra with increased optical density, which correlates to a high yield and smaller size. Also, the results of zeta potential, XRD, PCCS analysis showed the surface charge of -54.29 ±4.96 mV (AgNP-S), -42.64 ±3.762 mV (AgNP-F), -46.02 ±4.17 mV (AgNP-W), the crystallite size of 36 nm (AgNP-S), 13 nm (AgNP-F), 14 nm (AgNP-W) with face-centered cubic structure and average grain size of approximately 100 nm. Another important characteristic, such as elemental composition and constituent capping agent has been determined by EDX and FTIR. The silver nanoparticles were composed of ~80% Ag, ~15% K, and ~7.5% Ca (or ~2.8% P) elements. Moreover, the results of the FTIR measurement suggested that AgNP-F and AgNP-S contained distinct functional groups, on the other hand, AgNP-W contained all of the functional groups present in AgNP-F and AgNP-S. The silver nanoparticles showed antibacterial activity on both gram-negative bacterium *Escherichia coli* (5.5 ± 0.2 mm to 6.5 ± 0.3 mm) and gram-positive bacterium *Micrococcus luteus* (7 ± 0.4 mm to 7.7 ± 0.5 mm). Our study is meaningful as a first observation indicating the possibility of using special plant organs to control the characteristics of nanoparticles.

Introduction

Nanotechnology is a science that deals with the manipulation and fabrication of a nanoparticle [1] where at least one or two dimensions are within the range of 100 nm or less [2]. The nanometer-scaled particles have a unique property that differs them from their counterpart bulk material [3], their small size offers a large surface-to-volume ratio which causes a substantial biochemical and catalytic activity compared to the particles with the same composition [1, 4]. Nanoparticles are employed in the areas of drug delivery, biomedical sciences, gene delivery, chemical industries, optics, mechanics, catalysis and etc. [5]. Among metal nanoparticles, silver nanoparticles (AgNP) garner much attention due to their strong antibacterial and anti-inflammation effect. AgNPs are utilized in various physical, biological and pharmaceutical fields, for instance, cream or ointment containing AgNPs are applied for burns and wound area in order to inhibit bacterial infection [6]. Although AgNP is integrated into many areas, the exact mechanism explaining the particle formation is not fully uncovered yet. The traditional method for the synthesis of AgNP is to use physical and chemical approach to produce nanoparticles with controlled and well-defined size and shape [7]. However, the use of toxic substances, high pressure, and energy such as laser ablation, hydrothermal synthesis, solvothermal synthesis, pyrolysis and inert gas condensation has brought a demand for more biologically compatible nanoparticle [8, 9]. In recent years the synthesis of AgNP through biological method has been studied intensely. The biological method offers nanoparticles with high yield and stability compared to the conventional physical and chemical approach [10]. AgNP can be biosynthesized by bacteria, fungi, yeast, actinomycetes, and plant, thus avoiding toxic substances and

enabling them for further use in the medical and pharmaceutical field [11]. In recent years, the application of plants for the synthesis of AgNP has gained significant attention. Plant-mediated synthesis of AgNP has many advantages, it can be obtained under ambient temperature with low cost and the process is relatively fast compared to the bacteria, where a long process of maintaining cell culture is required [12]. Plants contain a wide range of metabolite that can aid in reducing silver ion, stabilizing and capping AgNP [13], therefore the concentration and composition of AgNP will vary depending on the plant type [3]. This is especially the case for the medicinal plant as it is a rich source of a complex phytochemicals and antioxidants. The main antioxidants of medicinal plants are polyphenols, carotenoids, and vitamins. The medical plant displays a wide range of anti-inflammatory, antibacterial, antiviral, anti-aging, and anti-cancer activity [14]. In addition to polyphenols found in plants, there are other biomolecules responsible for reducing and capping AgNP [15], these include polysaccharides, aldehydes, ketones, proteins, enzymes, amino acids, and caffeine [16]. The complex biomolecules found in medical plants assist in the reduction of metal ions and stabilization of the nanoparticles into desired shape and size [17]. The plant-mediated synthesis of AgNP is relatively simple as it requires plant extract and silver salt, thereafter it undergoes a reduction process [18]. There are many reports published regarding a medicinal plant-mediated synthesis of AgNP, this includes *Gmelina aroberea* [19], *Tecomella undulata* [20], *Artemisia absinthium* [21], *Datura stramonium* [22], *Calliandra haematocephala* [23], *Carica papaya* [24] etc. *Carduus crispus* is a plant species of the family Asteraceae that can be found in Mongolia. The medicinal effect ranges from a stomachache, rheumatism, atherosclerosis to cancer. Due to its medical properties, it is broadly applied to Mongolian traditional medicine [25]. The main activity of *Carduus crispus* is coagulation, antioxidant and anticonvulsive activity [26]. According to the study done by Baumberger the major compounds detected in *Carduus crispus* are flavonoids and coumarins, also alkaloids saccharides, essential oil, rubber, lipids contained in small quantities [27]. There are no available reports on the synthesis of AgNP using *Carduus crispus* as the plant extract. The mechanism of action of AgNP is not yet completely understood, however there are several hypotheses available explaining the antibacterial activity, anti-inflammatory and anti-cancer. It is known that nanoparticle has a large surface area that either penetrates the cell or attaches itself to the cell wall [11], causing a disturbance in the membrane permeability making it porous [28], and this action leads to a leakage of cell content. Furthermore, with the appearance of pores on the membrane nanoparticles diffuse to the cell where it binds with sulfur and phosphorus-containing proteins, thus leading to the inactivation of proteins and DNA [17], Another hypothesis suggests that the antibacterial activity of AgNPs may result from the release of Ag^+ ions through the oxidation dissolution process. Silver ions oxidized from AgNP mainly interact with thiol groups of various enzymes and protein, thereby interfering with the respiratory chain and disrupting the bacterial cell wall. Silver ions also facilitate the generation of reactive oxygen species (ROS), which is considered the main cause for most cell death through the inactivation of DNA replication and ATP production [29]. The present study aimed to synthesize silver nanoparticles by medicinal plant *Carduus crispus* extracts and characterize the final product, finally evaluate their antibacterial activities.

Results And Discussion

UV-Vis spectra analysis and color change

The visual color change from pale yellow to dark brown in response to time can be seen as evidence of the reduction of silver ions to AgNP. The change in color of biosynthesized AgNP is due to the excitation of surface plasmon resonance (SPR). Several studies done on the synthesis of AgNP via medicinal plant suggest the absorption peak around 412–470 nm with the duration of synthesis from 4 hours till 24 hours, this includes medicinal plants, such as *Abutilon indicum, Aegle marmelos, Azadirachta indica, Calliandra haematocephala, Calotropis procera, Carica papaya, Helicteres isora, Lawsonia inermi, Leptadenia reticulate, Rheum palmatum, Tecomella undulata, Tagetes erecta, Urtica dioica*. The rate of color change from light yellow to dark brown varied in these studies, the earliest color change began within 1 hour and till 4 hours [4, 20, 23–24, 30–38]. Alternatively, different studies utilizing non-medicinal plants for the AgNP synthesis, such as *Allium cepa, Chenopodiastrum murale, Cyperus rotundus, Eleusin indica, Euphorbia hirta, Melastoma malabathricum, Musa acuminate, Pachyrhizus erosus, Rubus glaucus* exhibited absorption peak from 401–780 nm and synthesized for 72 hours till 14 days. The color change of AgNP synthesized via C. murale turned to brown color after incubating overnight [39–43]. The difference in color change rate might be due to the different properties of the plant, specifically, the medicinal plant contains a wide range of phytochemicals, such as flavonoids, polyphenols, terpenoids, etc [44]. that assist in the formation of silver nanoparticles. Iravani [5] et al. has reported in their studies that flavonoids, polyphenols, terpenoids, alkaloids, and proteins are the main constituents responsible for the reduction and stabilization of the silver nanoparticle. Figure 1 shows the results of the color change of the synthesized silver nanoparticle with different organs of *Carduus crispus*, such as stem, flower and the whole plant. It can be seen that different plant organs affected differently on the silver nanoparticle synthesis, and particularly whole plant extract facilitated better silver nanoparticle formation compared to the stem and flower extract. The synthesis of silver nanoparticles with whole plant extract exhibited a darker color change. The variation of the color change might be due to the different phytochemical content in the plant organs. Following the visual color change study, the formation and stability of silver nanoparticles synthesized with flower, stem, and whole plant of *Carduus crispus* were characterized using a UV-Vis spectrophotometer (Fig. 2). The results revealed that silver nanoparticles synthesized with whole plant (AgNP-W) exhibited higher absorption compared to silver nanoparticles synthesized using plant organs such as flower (AgNP-F) and stem (AgNP-S). The higher absorption is directly proportional to the higher yield of silver nanoparticles in colloidal solution [45]. Additionally, the size of the synthesized silver nanoparticle was studied by observing the shift of the absorption peak towards a longer or shorter wavelength [8, 46]. In Fig. 2b-d, silver nanoparticles were measured at various times, and according to our results, the AgNP-W exhibited blueshift compared to AgNP-F and AgNP-S, which can be interpreted as the formation of smaller-sized silver nanoparticles.

Zeta potential analysis

Zeta potential explains the stability, dispersion, and surface charge of the nanoparticles. The zeta potential greater than + 30 mV or less than − 30 mV indicates the high stability of nanoparticles in dry powder form [31]. The high negative value produces repulsion between similarly charged particles in

suspension, therefore, resisting aggregation [47]. Several studies were done on silver nanoparticle synthesis with a medicinal plant such as Pot*entilla fulgens, Alpinia calcarata, Pestalotiopsis micospora, Urtica dioica, Jatropha curcas* resulted in the zeta potential of -18mV, -19.4mV, -35.7mV, -24.1mV, and −23.4mV respectively [4, 6, 12, 47–48]. Our results showed that zeta potential of the synthesized AgNP-W, AgNP-S, AgNP-F had an average zeta potential of -46.0 2 ± 4.17 (AgNP-W), -54.29 ± 4.96 (AgNP-S) and −42.64 ± 3.762 (AgNP-F) (Table 1). The zeta potential of AgNP-S exhibited a higher average value compared to the AgNP-W and AgNP-F, this may be due to the presence of different phytochemicals in each sample that reduces and cap silver nanoparticles. The results of the zeta potential analysis suggest that silver nanoparticles synthesized with *Carduus crispus* exhibit high stability and against agglomeration. Figure 3 showed that zeta potential values of AgNP-W, AgNP-S, and AgNP-F fall within the normal distribution curve, which indicates that synthesized silver nanoparticles are fairly monodisperse.

Table 1
Average zeta potential and mobility of AgNP-W, AgNP-S and AgNP-F

	Average zeta potential	Average mobility
AgNP-W	-46.0 2 ± 4.17	-3.52 ± 0.31
AgNP-S	-54.29 ± 4.96	-4.19 ± 0.38
AgNP-F	-42.64 ± 3.762	-3.25 ± 0.28

FTIR spectral analysis of synthesized AgNP by *Carduus crispus*

The presence of the functional groups capping AgNP synthesized using *Carduus crispus* is analyzed by FTIR and shown in Fig. 4. The presence of various organic compounds in the plant reveals multiple peaks compared to the chemical method where only a few and strong peaks are displayed [50]. The results of our FTIR analysis revealed the presence of several functional groups in AgNP-W, AgNP-S, AgNP-F. Additionally, the functional groups in AgNP-F and AgNP-S were present in AgNP-W samples as well, this may be due to the various phytochemicals capping the silver nanoparticles that are found both in flower and stem of *Carduus crispus*. The strong characteristic bands at ~3418 cm^{-1} to 3429 cm^{-1} and 2361 cm^{-1} in all samples AgNP-S, AgNP-F, AgNP-W are assigned to the O-H stretching/N-H stretching of amides and 2361cm^{-1} to the C ≡ C stretching. Additionally, the weak band at ~1017 to 1022 cm^{-1} and ~828 cm^{-1} assigned to carbohydrates and –C = O bending were found in all samples AgNP-S, AgNP-F, and AgNP-W. C-O stretching is present in AgNP-F which was observed from the very strong band at 1353 cm^{-1}. The weak bands at 2922 cm^{-1} and 2857 cm^{-1} of CH_3 stretch of alkane/carboxylic acids present in AgNP-F and were absent in AgNP-S. The band detected at ~3418 cm^{-1} to 3429 cm^{-1} and 1618.35 cm^{-1} correspond to the presence of phenolic compounds and flavonoids, and the band found on 1021.35 cm^{-1}

indicates carboxylic acid, ester, and ether groups of proteins and metabolites that may be involved in the synthesis of nanoparticles [33]. Our results showed that a strong band detected at 1611 cm^{-1} and 1017 cm^{-1} from AgNP-F correspond to the presence of flavonoids and proteins. On the other hand, weak bands detected at ~1696 cm^{-1} to 1371 cm^{-1} correspond to alcohol, carboxylic acids, alkyl halides/carboxylic acids/ester, alkenes/alkyl halides/aromatics, alkynes/alkyl halides stretch that peaks found from AgNP-S. According to Baumberger [27] the major compounds detected in *Carduus crispus* are flavonoids and coumarins, in addition, alkaloids saccharides, essential oil, rubber, and lipids contained in small quantities which in line with the presence of flavonoids and phenolic compounds in our synthesized AgNP. AgNP-F and AgNP-S contained different functional groups that correspond to various compounds, and AgNP-F revealed that it has a strong correlation with flavonoids from *Carduus crispus*. The results are confirmed by FTIR and UV-Vis spectra analysis that these functional groups are responsible as the capping and reducing agents.

XRD, PCCS and SEM/EDX analysis

The crystalline nature of the synthesized AgNP was confirmed by X-Ray crystallography. The XRD pattern of the nanoparticles was analyzed with an XRD instrument and is finally shown in Fig. 5. Bragg reflection of the 2θ peaks was observed at 32.25˚ to 81.62˚ and corresponded to (111), (200), (220), (311), (222) plane lattice which can be indexed to the face-centered cubic crystal nature of the silver. The average crystallite size was calculated using the Scherrer equation. The average crystallite sizes were 13 nm (AgNP-F), 14 nm (AgNP-W) and 36 nm (AgNP-S). The results of our study are in line with other published literature, the crystal nature of the silver nanoparticles synthesized with Ta*getes erecta* [31], *Urtica dioica* [4], *Aegle marmelos* was face-centered cubic with diffraction peaks of (111), (200), (220), (311) respectively [34]. Photon Cross-correlation Spectroscopy is a technique that measures the average nanoparticle size (grain size) based on the Brownian motion. In Fig. 6, the average particle size of AgNP-W was approximately 100 nm. The difference between PCCS and XRD analysis lies in the measurement method of the particle, application of the Scherrer equation on XRD data gives the average crystallite size, specifically the size of a single crystal inside the particle or grain. The morphological and elemental analysis was done on Scanning Electron Microscope (SEM) and Energy Dispersive X-Ray Spectroscopy (EDX). The elemental composition of the synthesized silver nanoparticle was assessed using EDX spectroscopy (Table 2). The results in Fig. 7 showed that AgNP-W, AgNP-S, and AgNP-F contained silver and potassium elements together with several other elements that differed in AgNP-F and AgNP-S samples, i.e. AgNP-F included phosphorus 2.8 %, potassium 15.2 %, and AgNP-S had calcium 7.5 %, pottassium 15.5 % elements. In contrast, AgNP-W contained all the elements including the elements that differed in AgNP-F and AgNP-S. Interestingly, the silver element in AgNP-F had the highest content of 82% compared to AgNP-W and AgNP-S with a silver content of 79 % and 77 % respectively. Another observation on EDX analysis revealed that AgNP-W, AgNP-F, AgNP-S did not show the presence of nitrogen peak, this in dicates that traces ions from $AgNO_3$ are absent in the samples. The different composition of plant organs, such as stem, flower and whole could be the reason for the observed variability in EDX, color change, FTIR and UV-Vis absorption.

Table 2
Elemental composition of the synthesized silver nanoparticles by *Carduus cripus*

	Silver, %	Potassium, %	Calcium, %	Phosphorus, %	Chlorine, %
AgNP-W	77 ±1	15.1 ±0.5	2.8 ±0.1	1.2 ±0.1	3.9 ±0.21
AgNP-F	82 ±1	15.2 ±0.4	-	2.8 ±0.15	-
AgNP-S	77 ±1	15.5 ±0.5	7.5 ±0.2	-	-

Antibacterial activity

The antibacterial activity of silver nanoparticles was studied against pathogenic bacterial strains of gram-negative *E.coli* and gram-positive *M.luteus* using the well diffusion method (Fig. 8). Standard antibiotics such as Penicillin G and Chloramphenicol, plant extracts, $AgNO_3$ and distilled water were chosen as the control group. The results of the antibacterial activity showed that all synthesized silver nanoparticles had efficient antibacterial activity against both gram-negative *E.coli* and gram-positive *M.luteus* bacterial strains. The inhibition zone of AgNP-F, AgNP-W and AgNP-S against *E.coli* and *M.luteus* were 6.5 ±0.3, 6 ±0.2, 5.5 ±0.2 and 7.5 ±0.3, 7 ±0.2, 7.7 ±0.4 mm respectively. The plant extract and $AgNO_3$ did not reveal any antibacterial activity against both *E.coli* and *M.luteus*, which can be interpreted that AgNP-W, AgNP-F, and AgNP-S are solely responsible for the antibacterial activity. The mode of action of AgNPs against bacteria is not completely understood yet. However, several hypotheses are explaining the antibacterial activity of silver nanoparticle: (1) generation of reactive oxygen species; (2) release of Ag + ions from AgNPs denaturize proteins by bonding with sulfhydryl groups; (3) attachment of AgNPs on bacteria and subsequent damage to bacteria [4, 11, 24]. The multiple published reports on the antibacterial activity of silver nanoparticles against gram-negative and gram-positive bacteria showed that silver nanoparticles had a slight antibacterial activity on gram-positive bacteria [6, 22, 31, 36]. Interestingly, AgNP synthesized by *Carduus crispus* exhibited effective inhibition on both gram-positive and gram-negative bacteria which can be interpreted as the antibacterial activity of silver nanoparticles (AgNP-W, AgNP-F and AgNP-S) is not affected by the difference in the bacterial wall.

Conclusion

The synthesis of silver nanoparticles via the biological method, specifically the plant extracts provides a natural, eco-friendly, cost-effective, rapid synthesis of silver nanoparticles. The present study reports the synthesis of silver nanoparticles by the medicinal plant *Carduus crispus* for reducing silver ions and stabilizing the silver nanoparticles. It has been reported that medicinal plants are a rich source of phenolic compounds such as flavonoids and phenolic acids, etc. Additionally, plant organs contain different contents of phenolic compounds, therefore flower, stem, and whole plant of *Carduus crispus* were chosen for this study. Afterward, the synthesized silver nanoparticles were characterized using visual color change, UV-Vis spectroscopy, zeta potential, FTIR, XRD, PCCS, and SEM-EDX. The

characterization of AgNP-W, AgNP-F, and AgNP-S revealed that AgNP-W had a higher yield, synthesis rate, and smaller-sized silver nanoparticles. The zeta potential conveys the stability and the result of all the synthesized silver nanoparticles showed the zeta potential value of -46.0 2 ± 4.17 (AgNP-W), -54.29 ± 4.96 (AgNP-S), and − 42.64 ± 3.762 (AgNP-F) which indicates highly stable silver nanoparticles. The variation in zeta potential may be due to the different phytochemical properties of the plant. Thereafter, FTIR analysis was utilized to study the role of phytochemical properties in plants for the synthesis of silver nanoparticles, the results revealed that different functional groups in AgNP-F and AgNP-S were also present in AgNP-W samples as well. And based on the UV-Vis spectra analysis AgNP-W and AgNP-F had the highest absorbance compared to AgNP-S, therefore we can conclude that the functional groups present and coincided in both AgNP-F and AgNP-W may play a contributing role in capping and synthesis of silver nanoparticles, these include functional groups with bands at 2922.28 cm^{-1}, 2857.66 cm^{-1}, 1711.90 cm^{-1}, 1611.59 cm^{-1}, 1079.22 cm^{-1} and 1017.49 cm^{-1} which correspond to alkanes, carboxylic acids, ketones, alkenes, amides, esters/ethers/amides, alkyl halides. Furthermore, strong bands at 3418 cm^{-1} to 3429 cm^{-1}, 1618.35 cm^{-1} to 1611 cm^{-1}, and 1017 cm^{-1} correlates to flavonoids and phenolic compounds. The EDX analysis detected the following elements, these include silver, potassium, phosphorus in AgNP-F; silver, potassium, calcium, chloride, and phosphorus in AgNP-W; finally, silver, potassium, calcium in AgNP-S samples. The synthesized silver nanoparticles had an average crystallite sizes of 13 nm (AgNP-F), 14 nm (AgNP-W) and 36 nm (AgNP-S) with face-centered crystal structure. Although the method of synthesis varied to AgNP-F, AgNP-W, and AgNP-S, their antibacterial activity showed efficient inhibition on both gram-negative and gram-positive bacteria. Based on the results, we can conclude that silver nanoparticles synthesized by whole plant of *Carduus crispus* have a faster rate of synthesis, higher yield with a smaller size, and high antibacterial activity against both gram-negative and gram-positive bacteria. The overall results show that the effectiveness of the synthesis of the flower for AgNP appears similar to using whole plant. Additionally, we have shown that the process of synthesizing nanoparticles can be manipulated with specific organs of plant, for example particle size and synthesis duration, biological effect, etc. Our study is meaningful as a first observation indicating the possibility of using special plant organs to control the characteristics of nanoparticles. Morevover, further studies are required in this area.

Methods

Chemicals and plant

The *Carduus crispus* was collected from Khuder soums, Selenge province of Mongolia (GPS coordinates: N 49.641772, E 107.80935) and the taxonomy was determined by a botanist from National University of Mongolia. The *Carduus crispus* used for the study does not violate the local regulations of Mongolia, the permission for the plant collection was granted from the Ministry of Environment and Tourism of Mongolia. The collected plant specimen of *Carduus crispus* was deposited into the publicly available herbarium of National University of Mongolia with deposition number UBU0002509. The Silver Nitrate

($AgNO_3$) with ≥ 99.0% purity was purchased from Sigma Aldrich. All the other relevant reagents are up to the standard.

Preparation of plant extract

The whole plant was washed with tap water in order to remove the adhering dust and soil particles, followed by washing with distilled water. 100 ml of distilled water was added to 5 g of *Carduus crispus* and boiled for 15 minutes, then cooled at ambient temperature. Afterward, it was filtered by Whatman filter paper and centrifuged twice at 10’000 rpm to obtain a plant extract. Finally, the extract was ready for the synthesis of AgNP.

Synthesis of silver nanoparticle

The aqueous plant extract of *Carduus crispus* and $AgNO_3$ (1 mM) were mixed with the ratio of 1:16, then the solution was exposed to the daylight and the reaction took place at the various time at room temperature. In order to obtain silver nanoparticles in powdered form, the solution was vaporized on a vacuum evaporator, and the final product of AgNP was kept inside the oven at a temperature of 300°C for 4 hours.

Characterization of AgNP synthesized by *Carduus crispus*

AgNP was successfully synthesized by using *Carduus crispus*. A color change from pale yellow to colloidal dark brown indicated the formation of silver nanoparticles. UV-Vis spectra analysis offers an insight into the synthesis and stability of the AgNP. Formation of the biosynthesized AgNP was determined by the UV-Vis spectrophotometer (Shimadzu UV-2500PC Series) at 30 min, 1 hour, 2 hours, 3 hours, 4 hours, 6 hours, 12 hours, 24 hours and was carried out at 350–700 nm range. FTIR spectrum was recorded in the range of 500 to 4000 cm^{-1} through the potassium bromide powder method using FTIR spectrophotometer (Prestege-21, Shimadzu, Japan) for understanding the constituent capping and reducing agents of silver nanoparticles. Also, elemental composition of the synthesized silver nanoparticles was analyzed with an energy dispersive X-ray spectroscope instrument (TM-10000 with EDX). To identify the structural phase present in the AgNP, XRD was performed by XRD instrument (Shimadzu, Maxima-X-7000) operating at 40 kV with a current of 30 mA and Co-Ka radiation. And crystalline size was determined by the Scherrer equation. To understand the size distribution and surface charge, zeta potential (ZetaCompact, CAD Instruments, France) and PCCS (NANOPHOX NX0061 instrument, Sympatec GmbH, Germany) methods were used for dispersed nanoparticles of silver.

Determination of anti-bacterial activity using well diffusion method

The agar well diffusion method was used to study the antibacterial activity of the synthesized silver nanoparticle. Broth medium was used to subculture bacteria and was incubated at 37°C for 24 hours, afterwards, overnight cultures were taken and spread on the agar plates to cultivate a uniform microbial

growth plate. The bacterial strains were gram-negative *Escherichia coli* and gram-positive *Micrococcus luteus*. And silver nitrate, plant extract, antibiotics (Penicillin G against *Micrococcus luteus* and Chloramphenicol against *Escherichia coli*) were chosen as the control group for the study of antibacterial activity. Finally, the petri dishes were incubated for 24 hours at 37°C. In order to evaluate the antibacterial activity of the synthesized silver nanoparticle, the diameter of the inhibition zone was measured and compared with the control groups.

Statistical analysis

All experiments were performed at least three times, independently and data were analyzed by a Student's t-test, and a value of $p < 0.05$ was considered significant.

References

1. Rafique MS, Sadaf I, Rafique MS, Tahir MB. A review on green synthesis of silver nanoparticles and their applications. Artif Cells, Nanomedicine Biotechnol. 45(7), 1272-1291 (2017). doi: 10.1080/21691401.2016.1241792
2. Abdelghany T.M, Al-Rajhi Aisha M.H., Al Abboud Mohamed A, Alawlaqi M.M, Ganash Magdah A, Helmy Eman A.M, et al. Recent advances in green synthesis of silver nanoparticles and their applications: About Future Directions. A Review. Bionanoscience. 8(1), 5-16 (2018). doi: 10.1007/s12668-017-0413-3
3. Shah M, Fawcett D, Sharma S, Tripathy SK, Poinern GEJ. Green synthesis of metallic nanoparticles via biological entities. Materials (Basel). 8(11), 7278-7308 (2015). doi: 10.3390/ma8115377
4. Jyoti K, Baunthiyal M, Singh A. Characterization of silver nanoparticles synthesized using Urtica dioica Linn. leaves and their synergistic effects with antibiotics . J Radiat Res Appl Sci. 9(3), 217-227 (2016). doi: 10.1016/j.jrras.2015.10.002
5. Iravani S, Korbekandi H, Mirmohammadi S V., Zolfaghari B. Synthesis of silver nanoparticles: Chemical, physical and biological methods. Res Pharm Sci. 9(6), 385-406 (2014).
6. Khandel P, Shahi SK, Soni DK, Yadaw RK, Kanwar L. Alpinia calcarata: potential source for the fabrication of bioactive silver nanoparticles. Nano Converg. 5(1) (2018). doi: 10.1186/s40580-018-0167-9
7. Mounika KC, Venakatesh J, Manogna K, Paul AD. Biosynthesis and characterization of silver nanoparticles from tuber extract of Cyperus rotundus and study of its antibacterial activity. Res J Pharm Biol Chem Sci. 8(5), 378-387 (2017).
8. Bala A, Rani G. A review on phytosynthesis, affecting factors and characterization techniques of silver nanoparticles designed by green approach. Int Nano Lett. 10(3), 159-176 (2020). doi: 10.1007/s40089-020-00309-7
9. Rajendran R, Ganesan N, Balu SK, Alagar S, Thandavamoorthy P, Thiruvengadam D. Green synthesis, characterization, antimicrobial and cytotoxic effects of silver nanoparticles using Origanum Heracleoticum L. leaf extract. Int J Pharm Pharm Sci. 7(4):288-293 (2015).

10. Lee SH, Jun BH. Silver nanoparticles: Synthesis and application for nanomedicine. Int J Mol Sci. 20(4) (2019). doi: 10.3390/ijms20040865
11. Siddiqi KS, Husen A, Rao RAK. A review on biosynthesis of silver nanoparticles and their biocidal properties. J Nanobiotechnology. 16(1) (2018). doi: 10.1186/s12951-018-0334-5
12. Mittal AK, Tripathy D, Choudhary A, Choudhary A, Kumar Aili P, Chatterjee A, et al. Bio-synthesis of silver nanoparticles using Potentilla fulgens Wall. ex Hook. and its therapeutic evaluation as anticancer and antimicrobial agent. Mater Sci Eng C Mater Biol Appl. 53, 120-127 (2015). doi: 10.1016/j.msec.2015.04.038
13. Tashi T, Vishal Gupta N, Mbuya VB. Silver nanoparticles: Synthesis, mechanism of antimicrobial action, characterization, medical applications, and toxicity effects. J Chem Pharm Res. 8(2), 526-537 (2016).
14. Xu DP, Li Y, Meng X, Zhou T, Zhou Y, Zheng Jie, et al. Natural antioxidants in foods and medicinal plants: Extraction, assessment and resources. Int J Mol Sci. 18(1), 20-31 (2017). doi: 10.3390/ijms18010096
15. Review M. A review on green silver nanoparticles based on plants : Synthesis , potential applications and eco-friendly approach. International Food Research Journal. 23(2), 446-463 (2016).
16. Yaqoob AA, Umar K, Ibrahim MNM. Silver nanoparticles: various methods of synthesis, size affecting factors and their potential applications–a review. Appl Nanosci. 10(5), 1369-1378 (2020). doi: 10.1007/s13204-020-01318-w
17. Vijayan R, Joseph S, Mathew B. Green synthesis, characterization and applications of noble metal nanoparticles using Myxopyrum serratulum a. W. Hill leaf extract. Bionanoscience. 8(1), 105-117 (2018). doi: 10.1007/s12668-017-0433-z
18. Natsuki J. A review of silver nanoparticles: synthesis methods, properties and applications. Int J Mater Sci Appl. 4(5), 325 (2015). doi: 10.11648/j.ijmsa.20150405.17
19. Saha J, Begum A, Mukherjee A, Kumar S. A novel green synthesis of silver nanoparticles and their catalytic action in reduction of Methylene Blue dye. Sustain Environ Res. 27(5), 245-250 (2017). doi: 10.1016/j.serj.2017.04.003
20. Chaudhuri SK, Chandela S, Malodia L. Plant mediated green synthesis of silver nanoparticles using Tecomella undulata leaf extract and their characterization. Nano Biomed Eng. 8(1), 1-8 (2016). doi: 10.5101/nbe.v8i1.p1-8
21. Ali M, Kim B, Belfield KD, Norman D, Brennan M, Ali GS. Green synthesis and characterization of silver nanoparticles using Artemisia absinthium aqueous extract - A comprehensive study. Mater Sci Eng C. 58, 359-365 (2016). doi: 10.1016/j.msec.2015.08.045
22. Gomathi M, Rajkumar PV, Prakasam A, Ravichandran K. Green synthesis of silver nanoparticles using Datura stramonium leaf extract and assessment of their antibacterial activity. Resour Technol. 3(3), 280-284 (2017). doi: 10.1016/j.reffit.2016.12.005
23. Raja S, Ramesh V, Thivaharan V. Green biosynthesis of silver nanoparticles using Calliandra haematocephala leaf extract, their antibacterial activity and hydrogen peroxide sensing capability.

Arab J Chem. 10(2), 253-261 (2017). doi: 10.1016/j.arabjc.2015.06.023

24. Banala RR, Nagati VB, Karnati PR. Green synthesis and characterization of Carica papaya leaf extract coated silver nanoparticles through X-ray diffraction, electron microscopy and evaluation of bactericidal properties. Saudi J Biol Sci. 22(5), 637-644 (2015). doi: 10.1016/j.sjbs.2015.01.007
25. Davaakhuu G, Sukhdolgor J, Gereltu B. Lipid lowering effect of ethanolic extract of *carduus crispus* l. On hypercholesterolemic rats. Mong J Biol Sci. 8(2), 49-51 (2010). doi: 10.22353/mjbs.2010.08.14
26. Awobajo FO, Adegoke O, Odugbemi TO. Phytochemical and antimicrobial screening of hybanthus enneaspermus and paquetina nigricense. Recent Research in Science and Technology. 1(4), 159-160 (2009).
27. Baumberger J, Brantner A, Kunert O, Bucar F. Phytochemical and biological investigations on *Carduus crispus L*. Planta Medica. 76(12) (2010). doi: 10.1055/s-0030-1264365
28. Espoir K. Kambale, Christian I. Nkanga, Blaise-Pascal. Mutonkole, Alain M. Bapolisi, Daniel O. Tassa, Jean-Marie I. Liesse, et al. Green synthesis of antimicrobial silver nanoparticles using aqueous leaf extracts from three Congolese plant species (Brillantaisia patula, Crossopteryx febrifuga and Senna siamea). Heliyon. 6(8), e04493 (2020). doi: 10.1016/j.heliyon.2020.e04493
29. Liao C, Li Y, Tjong SC. Bactericidal and cytotoxic properties of silver nanoparticles. Int J Mol Sci. 20(2) (2019). doi: 10.3390/ijms20020449
30. Arokiyaraj S, Vincent S, Saravanan M, Lee Y, Oh YK, Kim KH. Green synthesis of silver nanoparticles using Rheum palmatum root extract and their antibacterial activity against Staphylococcus aureus and Pseudomonas aeruginosa. Artif Cells, Nanomedicine Biotechnol. 45(2), 372-379 (2017). doi: 10.3109/21691401.2016.1160403
31. Padalia H, Moteriya P, Chanda S. Green synthesis of silver nanoparticles from marigold flower and its synergistic antimicrobial potential. Arab J Chem. 8(5), 732-741 (2015). doi: 10.1016/j.arabjc.2014.11.015
32. Mujeeb Khan, Mohammed Rafi Shaik, Syed Farooq Adil, Shams Tabrez Khan, Abdulrahman Al-Warthan, Mohammed Rafiq H. Siddiqui, et al. Plant extracts as green reductants for the synthesis of silver nanoparticles: lessons from chemical synthesis. Dalt Trans. 47(35), 11988-12010 (2018). doi: 10.1039/C8DT01152D
33. Rani Mata, Jayachandra Reddy Nakkala, Sudha Rani Sadras. Biogenic silver nanoparticles from Abutilon indicum: Their antioxidant, antibacterial and cytotoxic effects in vitro. Colloids Surf B Biointerfaces. 128, 276-286 (2015). doi: 10.1016/j.colsurfb.2015.01.052.
34. Krupa AND, Raghavan V. Biosynthesis of silver nanoparticles using aegle marmelos (bael) fruit extract and its application to prevent adhesion of bacteria : a strategy to control microfouling. Bioinorg Chem Appl. 2014, 949538 (2014). doi: 10.1155/2014/949538.
35. Annamalai P, Balashanmugam P, Kalaichelvan PT. Biogenic synthesis silver nanoparticles using peltophorum pterocarpum leaf extracts and its antimicrobial efficacy against selective pathogens. Int J Appl Pharm. 10(6), 112-118 (2018). doi: 10.22159/ijap.2018v10i6.28573

36. Mohamed NH, Ismail MA, Abdel-Mageed WM, Shoreit AAM. Antimicrobial activity of latex silver nanoparticles using Calotropis procera. Asian Pac J Trop Biomed. 4(11), 876-883 (2014). doi: 10.12980/APJTB.4.201414B216
37. Bhakya S, Muthukrishnan S, Sukumaran M, Muthukumar M. Biogenic synthesis of silver nanoparticles and their antioxidant and antibacterial activity. Appl Nanosci. 6(5), 755-766 (2016). doi: 10.1007/s13204-015-0473-z
38. Kumara Swamy M, Sudipta KM, Jayanta K, Balasubramanya S. The green synthesis, characterization, and evaluation of the biological activities of silver nanoparticles synthesized from Leptadenia reticulata leaf extract. Appl Nanosci. 5(1), 73-81 (2015). doi: 10.1007/s13204-014-0293-6
39. Sharma P, Pant S, Rai S, Yadav RB, Sharma S, Dave V. Green synthesis and characterization of silver nanoparticles by Allium cepa L. to produce silver nano-coated fabric and their antimicrobial evaluation. Appl Organomet Chem. 32(3), 1-13 (2018). doi: 10.1002/aoc.4146
40. Abdel-Aziz MS, Shaheen MS, El-Nekeety AA, Abdel-Wahhab MA. Antioxidant and antibacterial activity of silver nanoparticles biosynthesized using Chenopodium murale leaf extract. J Saudi Chem Soc. 18(4), 356-363 (2014). doi: 10.1016/j.jscs.2013.09.011
41. Syafiuddin A, Salmiati, Hadibarata T, Beng Hong Kueh A, Razman Salim M. Novel weed-extracted silver nanoparticles and their antibacterial appraisal against a rare bacterium from river and sewage treatment plan. Nanomaterials. 8(1) (2014). doi: 10.3390/nano8010009
42. Sahni G, Panwar A, Kaur B. Controlled green synthesis of silver nanoparticles by Allium cepa and Musa acuminata with strong antimicrobial activity. Int Nano Lett. 5(2), 93-100 (2015). doi: 10.1007/s40089-015-0142-y
43. Kumar B, Smita K, Cumbal L, Debut A. Green synthesis of silver nanoparticles using Andean blackberry fruit extract. Saudi J Biol Sci. 24(1), 45-50 (2017). doi: 10.1016/j.sjbs.2015.09.006
44. Chung IM, Park I, Seung-Hyun K, Thiruvengadam M, Rajakumar G. Plant-Mediated Synthesis of Silver Nanoparticles: Their characteristic properties and therapeutic applications. Nanoscale Res Lett. 11(1), 1-14 (2016). doi: 10.1186/s11671-016-1257-4
45. Aoife C. Power, Anthony J. Betts, John F. Cassidya. Non aggregated colloidal silver nanoparticles for surface enhanced resonance Raman spectroscopy. Analyst. 136, 2794 (2011). doi: 10.1039/C1AN15250E
46. Saion E, Gharibshahi E, Naghavi K. Size-controlled and optical properties of monodispersed silver nanoparticles synthesized by the radiolytic reduction method. Int J Mol Sci. 14(4), 7880-7896 (2013). doi: 10.1039/C1AN15250E
47. Jorge de Souza TA, Rosa Souza LR, Franchi LP. Silver nanoparticles: An integrated view of green synthesis methods, transformation in the environment, and toxicity. Ecotoxicol Environ Saf. 171, 691-700 (2019). doi: 10.1016/j.ecoenv.2018.12.095
48. Netala VR, Bethu MS, Pushpalatha B, Baki VB, Aishwarya S, Rao JV. Biogenesis of silver nanoparticles using endophytic fungus Pestalotiopsis microspora and evaluation of their antioxidant and anticancer activities. Int J Nanomedicine. 11, 5683-5696 (2016). doi: 10.2147/IJN.S112857

49. Chauhan N, Tyagi AK, Kumar P, Malik A. Antibacterial potential of Jatropha curcas synthesized silver nanoparticles against food borne pathogens. Front Microbiol. 7, 1-13 (2016). doi: 10.3389/fmicb.2016.01748
50. Akinsiku A. Green synthesis of capped silver nanoparticles and their hybrids : antimicrobial and optical properties by akinsiku anuoluwa abimbola. Covenant University (2017). http://eprints.covenantuniversity.edu.ng/9513/

Figures

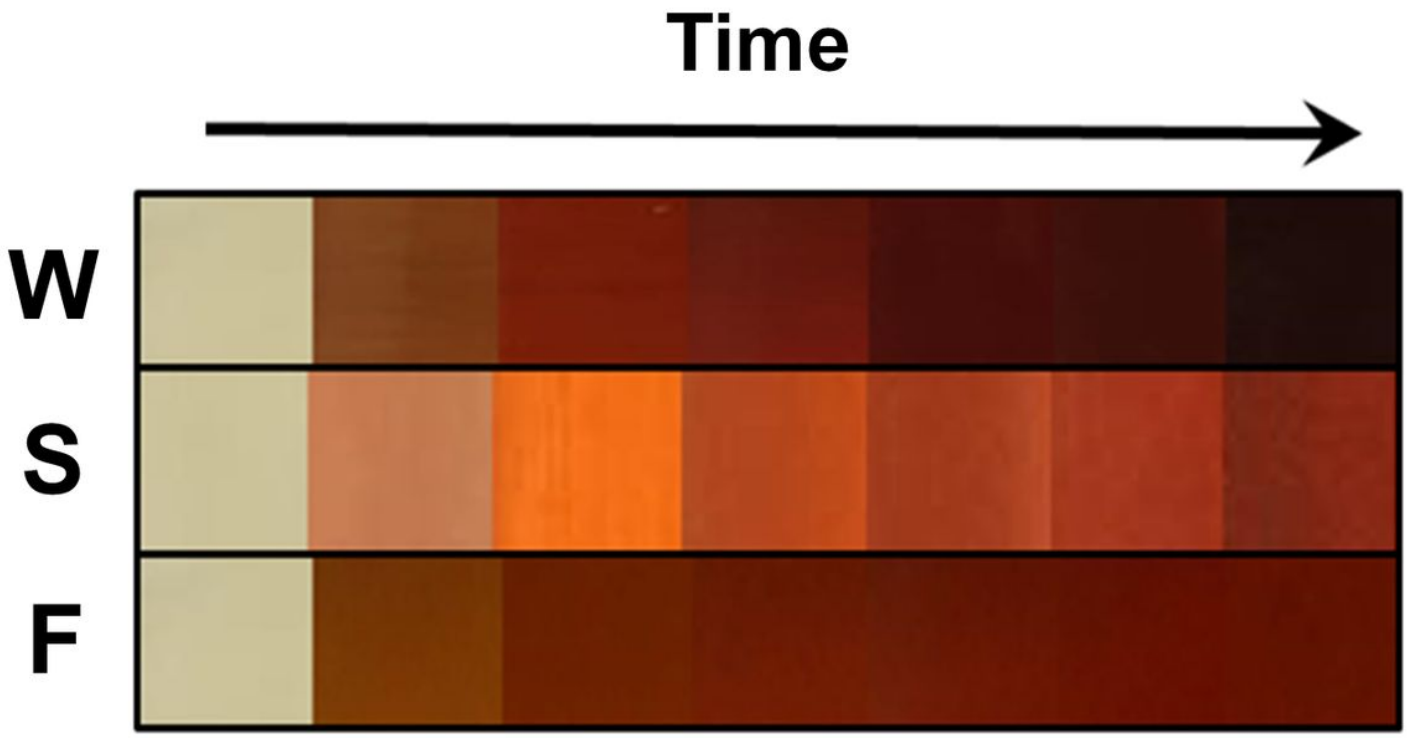

Figure 1

Color changes in biosynthesized silver nanoparticle with different parts of Carduus crispus. S-stem, F-flower and W-whole plant.

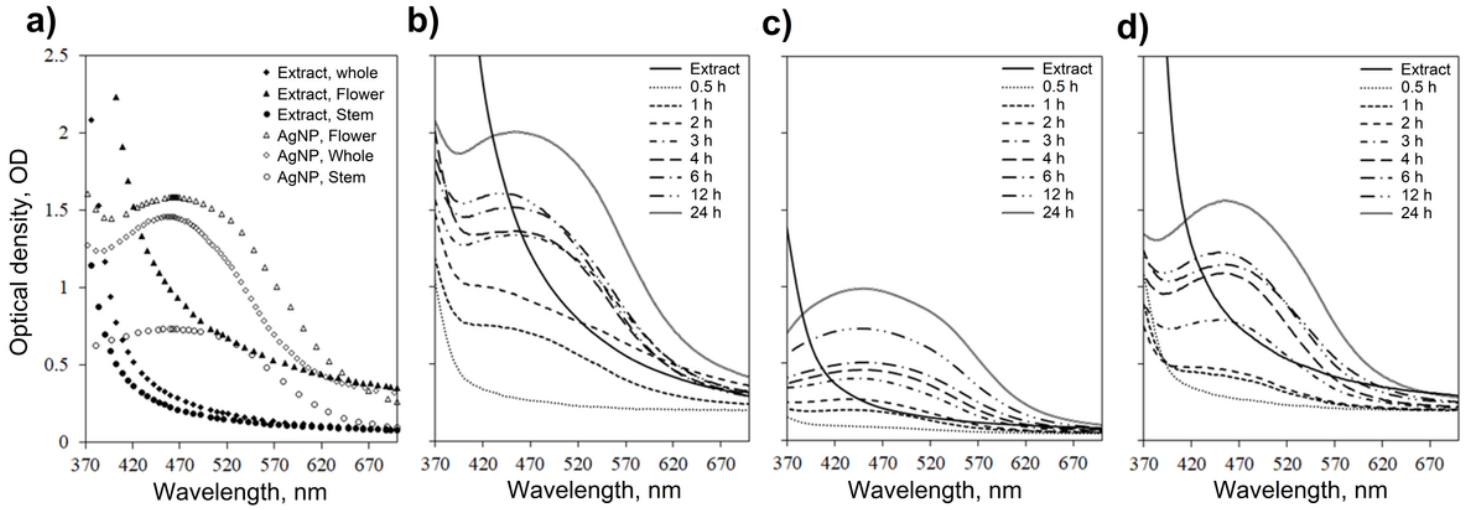

Figure 2

UV–Vis spectra for the reaction mixture containing of silver nanoparticles synthesized from Carduus crispus flower (AgNP-F), stem (AgNP-S) and whole plant (AgNP-W). Shown are the UV–Vis absorption spectra from 370 to 700 nm of all plant organs and synthesized (a) AgNPs, (b) AgNP-W, (c) AgNP-S, and (d) AgNP-F

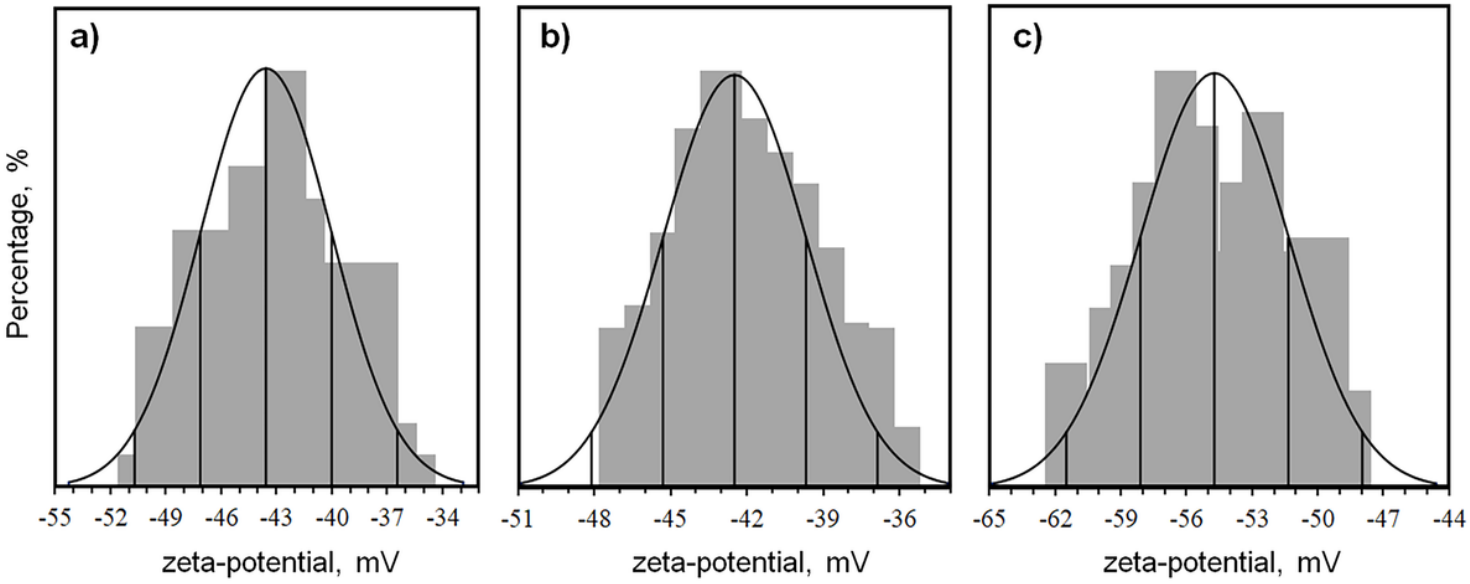

Figure 3

Zeta potential analysis of (a) AgNP-W, (b) AgNP-F and (c) AgNP-S

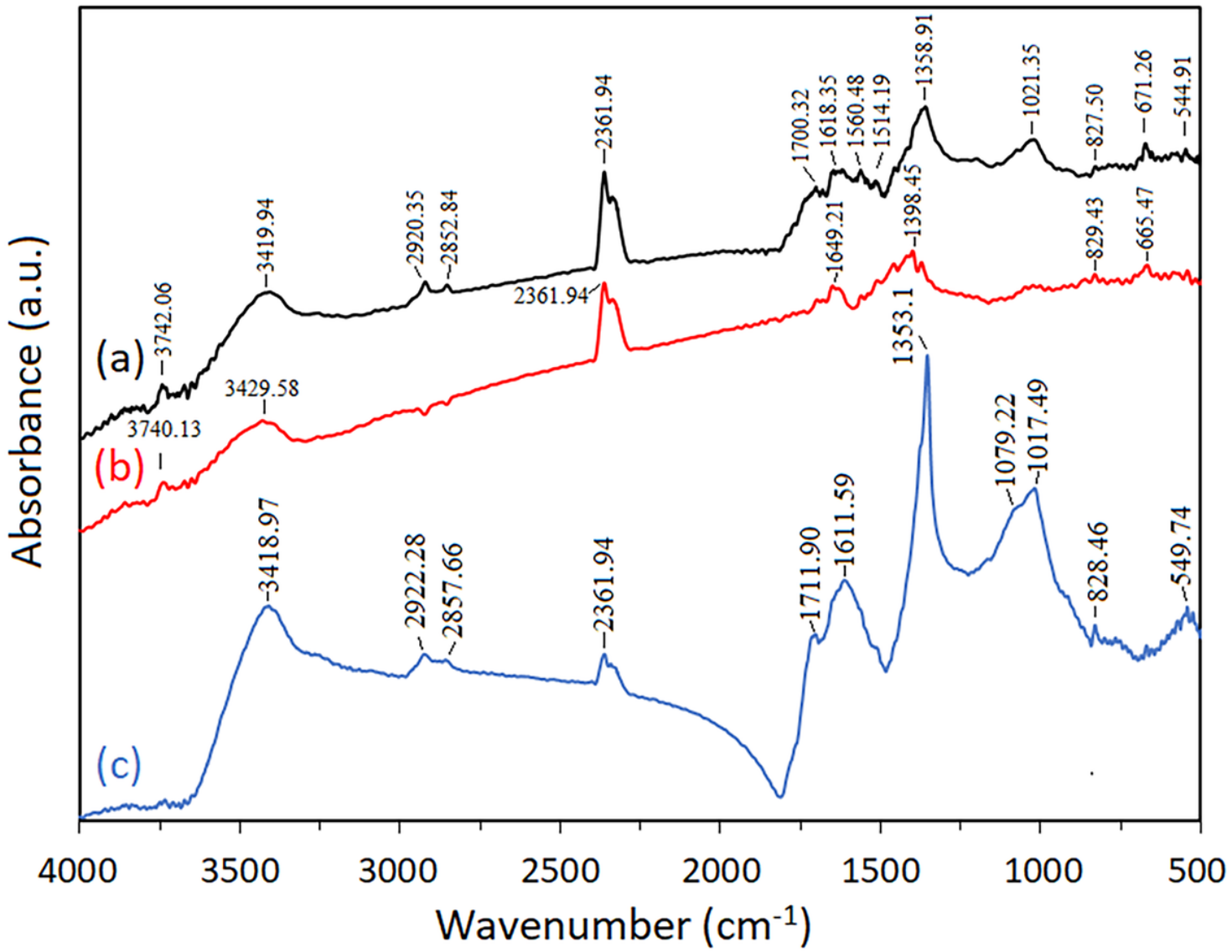

Figure 4

Fourier transform infrared spectra of (a) AgNP-W, (b) AgNP-S, and (c) AgNP-F.

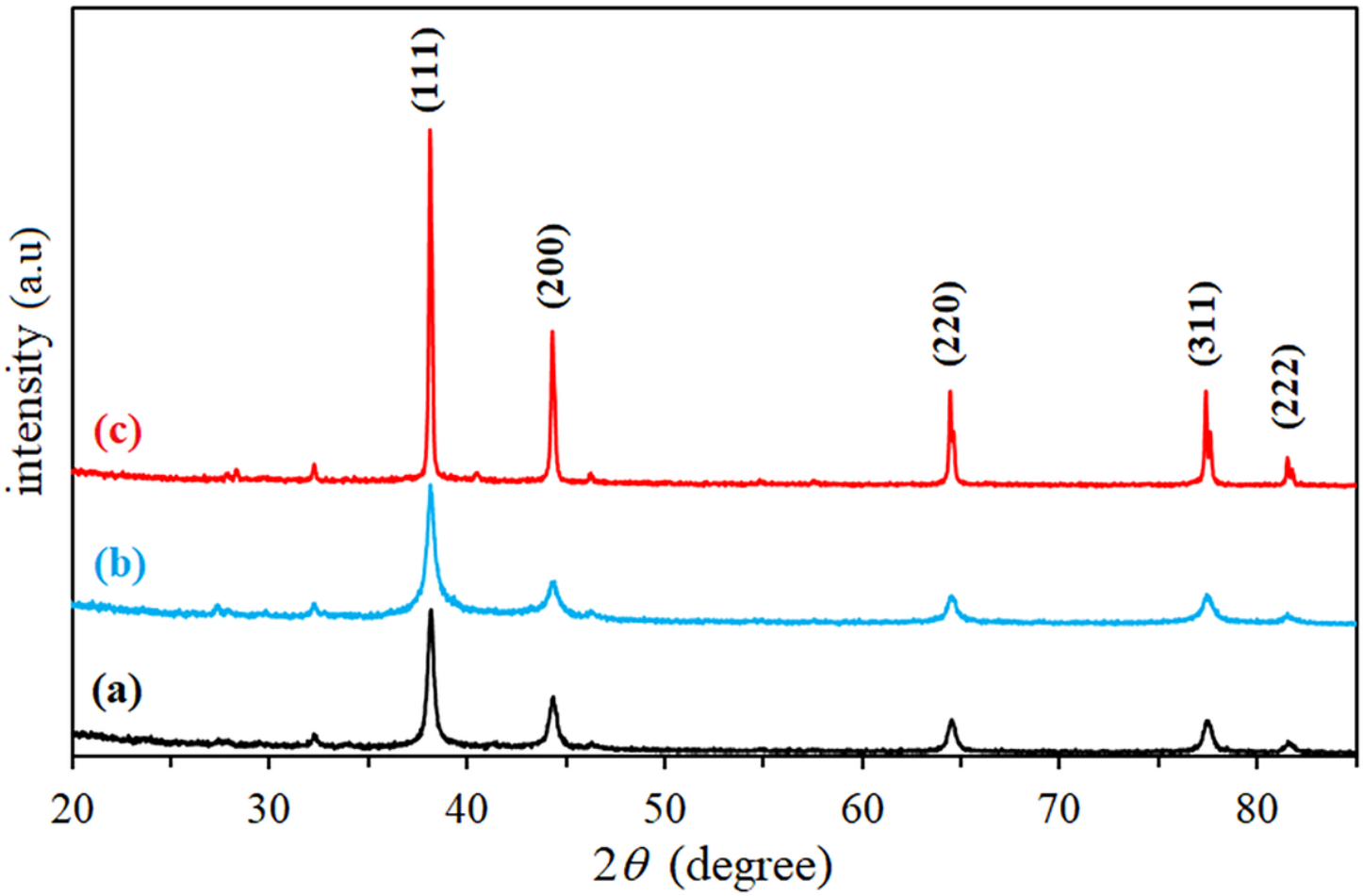

Figure 5

XRD spectra of (a) AgNP-W, (b) AgNP-F, (c) AgNP-S. Peaks are appeared at 111, 200, 220, 311 and 222.

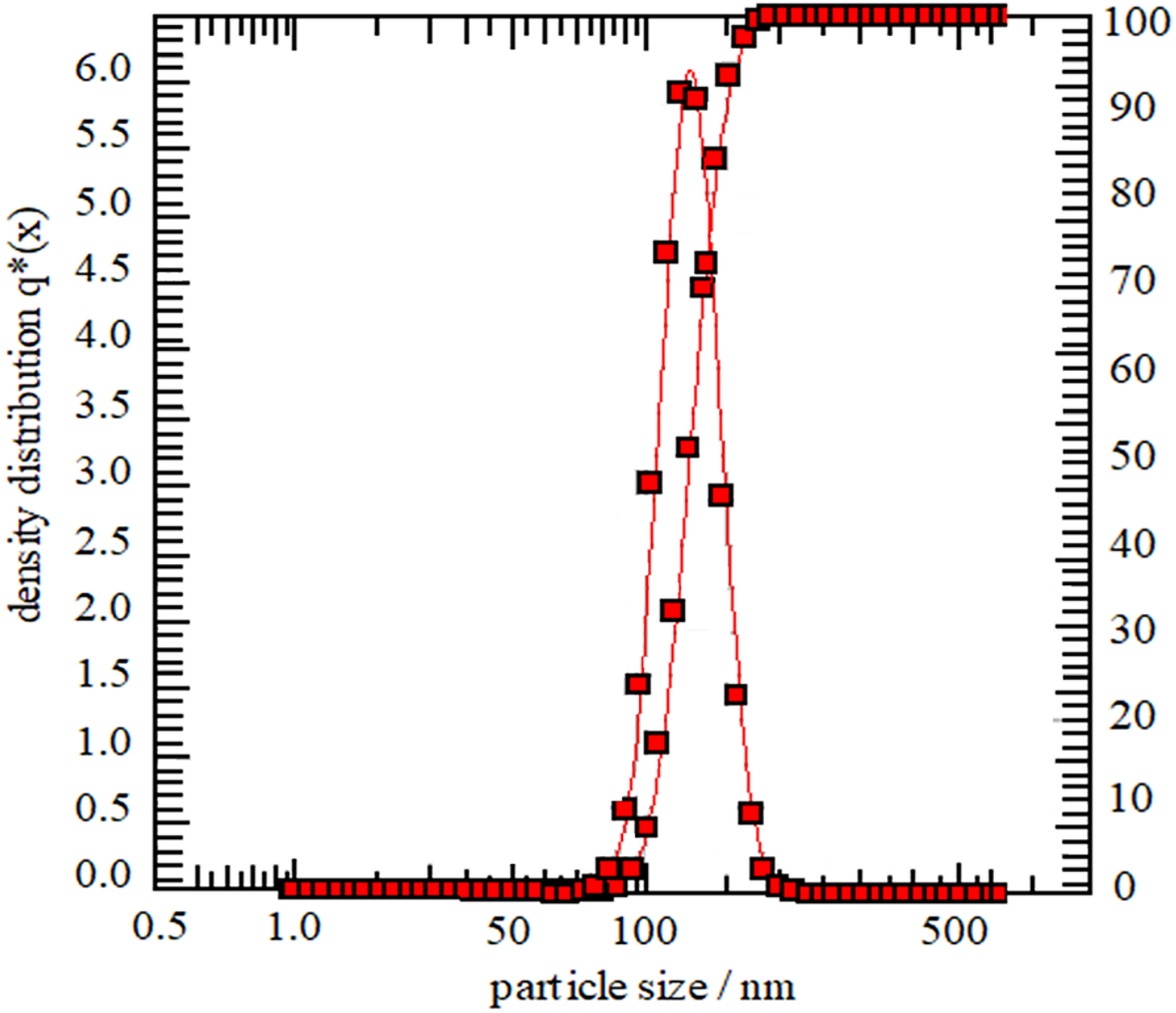

Figure 6

Particle number distribution of synthesized AgNP by Carduus crispus.

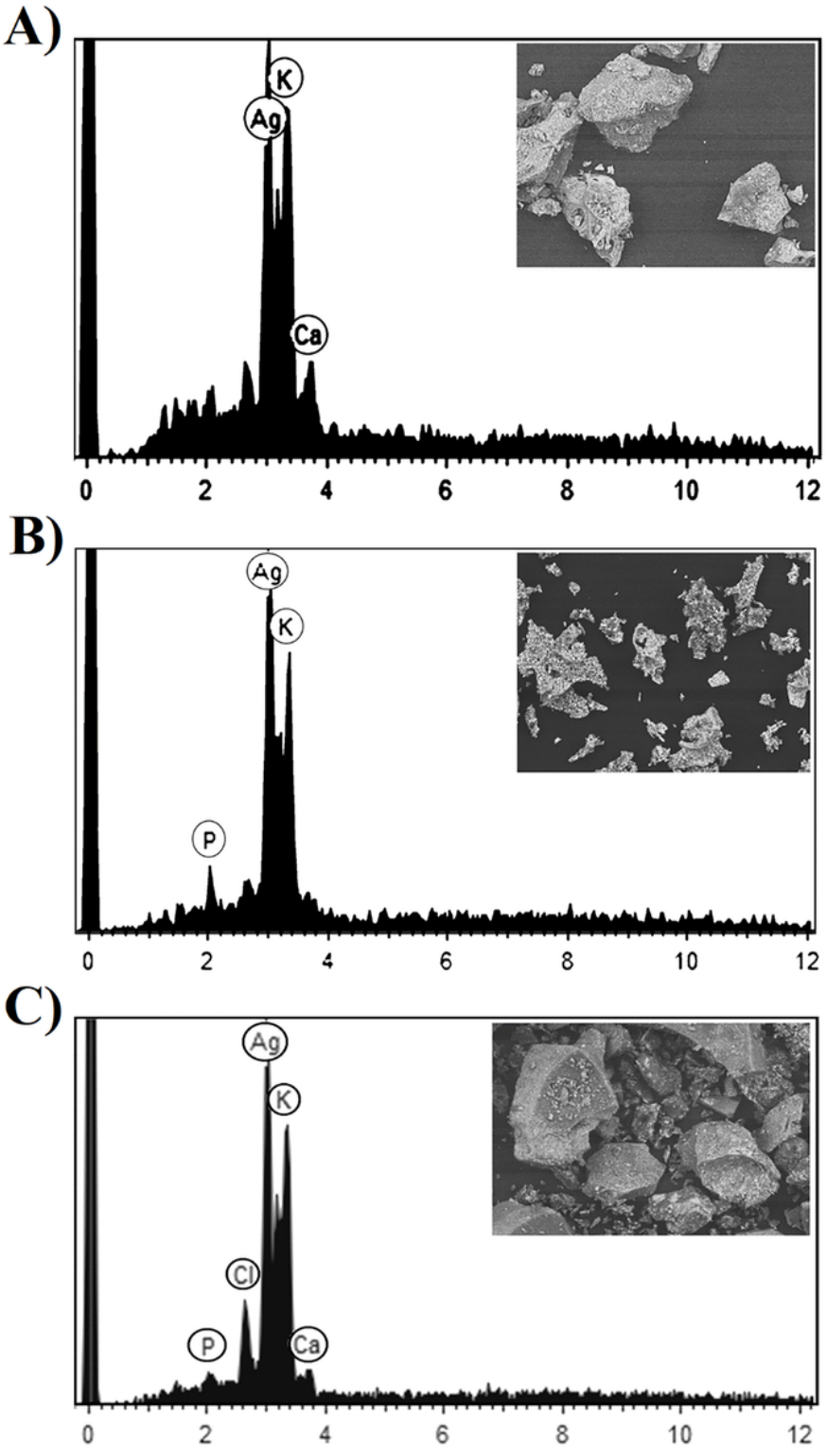

Figure 7

EDX spectra for (a) AgNP-F, (b) AgNP-S and (c) AgNP-W along with SEM image area (inset).

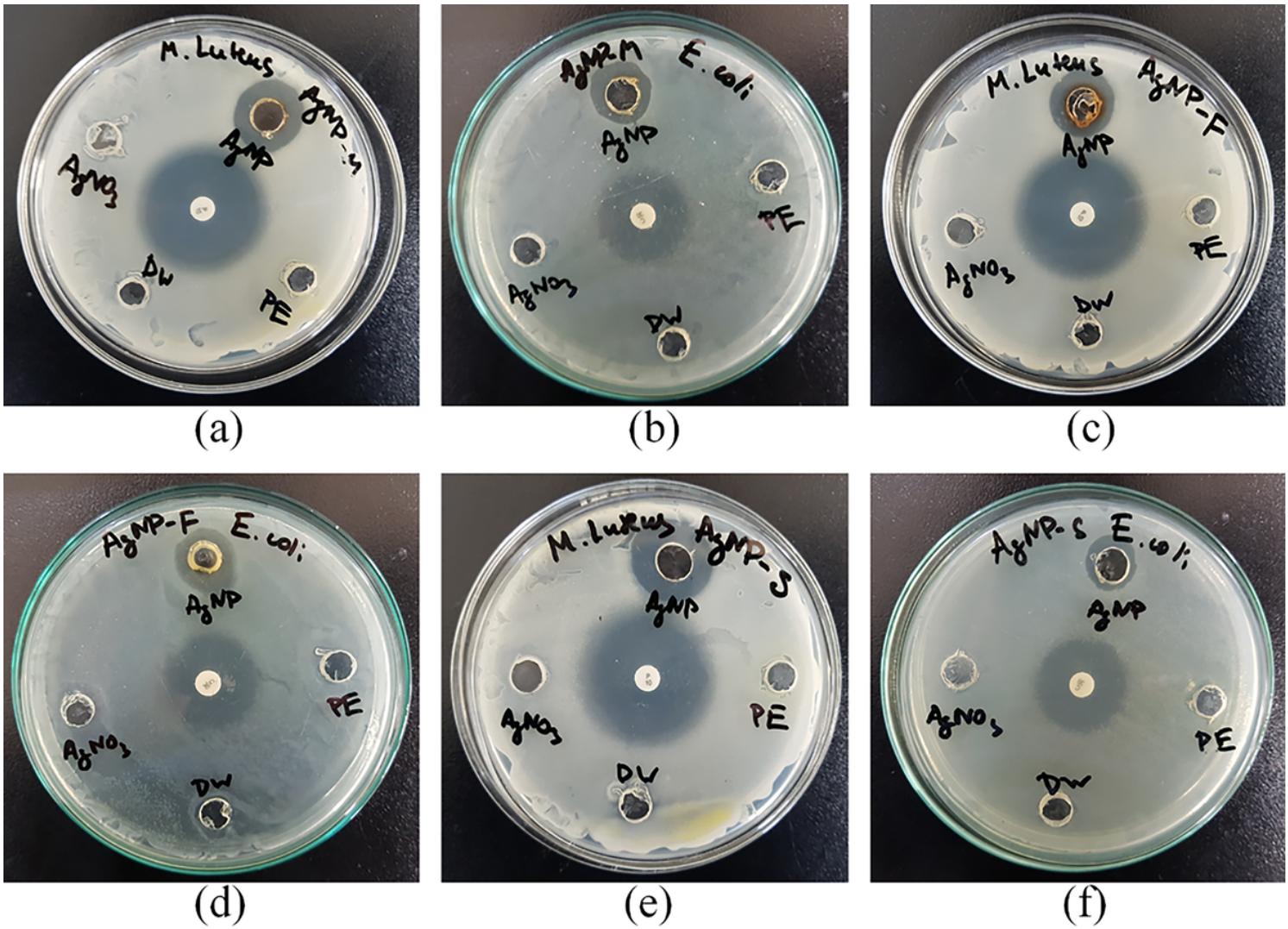

Figure 8

Petri dishes showing the zone of inhibition of synthesized AgNP-W on (a) M. luteus and (b) E. coli, and AgNP-F on (c) M. luteus and (d) E. coli, AgNP-S on (e) M. luteus and (f) E. coli (AgNP: silver nanoparticle, AgNO3: silver nitrate, DW: distilled water, PE: plant extract).